SUPPORTING INFORMATION

Title: Processed bamboo as a novel formaldehyde-free high-performance furniture bio-composite

Authors: Shengbo Ge[a,b#], Nyuk Ling Ma[c#], Shuaicheng Jiang[b#], Yong Sik Ok[d,#], Su Shiung Lam[e,a*], Cheng Li[a], Sheldon Qiang Shi[f], Xu Nie[g], Ying Qiu[g], Dongli Li[b], Qingding Wu[b], Daniel C.W. Tsang[h], Wanxi Peng[a,b*], Christian Sonne[i,a*]

Corresponding author: cs@bios.au.dk

This includes:

Extended Materials and Methods

FT-IR analysis

The FT-IR spectra of the samples were obtained by a FT-IR spectrophotometer (IR100) using KBr discs containing 1.00% finely ground sample. This analysis was used to explain the changes in molecular structure and internal functional groups during the conversion of the natural bamboo into bio-composite. The FT-IR spectra of the samples were obtained on an FT-IR spectrophotometer (IR100) using KBr discs containing 1.00% finely ground sample. The samples were prepared by mixing with potassium bromide (ratio 1 : 7) using pestle and mortar, and then subjected to FTIR analysis at spectra ranging from 400 to 4000 cm^{-1}.

TGA analysis

TGA was performed using a TG20 Thermal Gravimetric Analyzer (209-F1 TG, Netzsch, Germany) to investigate the proximate content (e.g., moisture, volatile matter), thermal stability, reaction kinetics, and stages of decomposition occurred during conversion of the natural bamboo into a bio-composite. TGA was performed by heating 10 mg of samples at a heating rate of 20 °C/min from room temperature to 750 °C with nitrogen gas (N_2) as carrier gas at a flow rate of 40 ml/min.

Cone calorimeter analysis

Cone Calorimetry was performed according to the ISO 5660-1 standard method. The heat released was measured using a dual cone calorimeter from Fire Testing Technology Ltd.. The setup, calibration, and measurements were in accordance with the ISO 5660-1 standard method [15]. Samples were mounted horizontally by using a specimen holder with edge frame. The bottom of the holder was lined with a ceramic fiber blanket. The bottom and sides of each sample were wrapped

with a 0.02-mm-thick aluminum foil. The heat release calculations were based on the measurement of oxygen, carbon monoxide, and carbon dioxide concentrations in the dried exhaust gas. Duplicate tests were conducted at heat fluxes of 30 and 50 kW/m^2. Samples were prepared by cutting a bamboo bio-composite (70 mm thick) into 50 mm × 50 mm square pieces.

XRD analysis

X-ray diffractograms (XRD) are used to measure and analyze the cellulose crystallinity of the bamboo fiber and bamboo bio-composite, and the results are presented in Fig. S-2 [16, 17]. I_{am} is the diffracted intensity of the peak detected at $2\theta = 16.0°$ in the amorphous region, and I_{002} is the intensity of the peak detected at $2\theta = 22.0°$ in the crystal region. Cr is the relative crystallinity and can be determined from $Cr = (I_{002} - I_{am})/I_{002} \times 100\%$. The X-ray diffraction patterns of samples were observed on a XD-2 diffractometer (General Analysis of Beijing General Instrument Co., Ltd., Beijing, P.R. China) with Cu-Kα radiation ($\lambda = 1.5406$ Å) to investigate the microstructure of the sample and determine the crystallinity that influences the properties of the sample. The X-ray tube used was a Cu tube with 36 kV of pipe potential and 20 mA of pipe current, and $2\theta/\theta$ continuous scanning was used as the method for measurement. A graphite crystal monochromator was used with the slit device set at DS = 1°, SS = 1°, RS = 0.3 mm. The rotary half-cone angle 2θ was from 5 to 42° with 2°/min of scanning velocity and 0.01 of scan step angle.

Cellulose crystallinity was calculated according to equation (1) as follows:

$$Cr = (I_{002} - I_{am})/I_{002} \times 100\%, \quad (1)$$

where Cr is the relative percentage of crystallinity, I_{002} is the intensity of the peak at 002 of the crystal region, and I_{am} is the diffracted intensity of the peak at $2\theta = 18°$ in the amorphous region.

SEM analysis

The scanning electron microscope is a new type of electronic optical instrument. It has features such as simple sample preparation, wide adjustable zoom range, high image resolution, and large depth of field [18]. For decades, SEM has been widely used in the fields of biology, medicine, metallurgy, and other disciplines, which has promoted the development of various related disciplines and has made great contributions to the analysis of the structure and morphology of materials in particular [19,20]. A scanning electron microscope (Hitachi SU6600 microscope) was used to determine the surface morphology of the samples at 10 kV of accelerating voltage. This allowed the investigation of the microstructure, pore size, grain boundary, and degree of agglomeration of the samples. The sample's surface was coated in a vacuum evaporator with a thin film of Au and then placed in the sample SEM chamber for analysis.

Nanoindentation tests

Nanoindentation possesses high resolution and depth sensing ability. It has become an important tool in measurements of nanomechanical properties for small scale materials [21,22]. Nanoindentation is widely used to measure micromechanical properties of materials [23]. Owing to the small sample volume under nanoindentation, the test can be highly localized to a specific microstructural feature [24]. Nanoindentation tests were performed on a Hysitron TI-950 TriboIndenter to determine the hardness of the samples. This testing also includes the Young's modulus test of the samples, which can be used to investigate the contact stiffness, creep, elastic work, plastic work, fracture toughness, stress-strain curve, fatigue, storage modulus, and loss modulus. A nano-DMA transducer with a Berkovich probe and a trapezoidal load function was used for standard quasistatic indentation testing. A peak load of 1000 μN was used, and the test results were calculated by the curve of force and indentation depth.

Micro CT analysis

The microstructures of the samples were analyzed using a SkyScan 1172 X-ray micro-computed tomography (micro-CT) (Bruker Corp., USA). It is a device that uses X-ray to scan the sample and then convert the signal into tomographic images that can clearly demonstrate the differences in the internal structure of the material. A source voltage of 60 kV and current of 167 μA were selected to obtain the optimum attenuation contrast. A set of 1202 projections was obtained without filter at an angular step size of 0.3° and a 2 K binning mode (with a resolution of 2000 × 1336 pixels). The corresponding spatial resolution of the X-ray radiography was about 8.49 μm/pixel. NRexon software was employed to perform the reconstruction of the 3D object, and Data Viewer and CTvox were used for data analysis and visualization.

Although it cannot provide all the data of a standard analysis, micro-CT has substantial potential advantages in trying to determine volume ratio of fibers and volume ratio of interfaces in 3D [25,26]. Micro-CT has been shown to provide fast and nondestructive characterization and measurement of the 3D properties of a scaffold [27,28] or tissue-engineered construct [29,30].

Extended Data and Figures

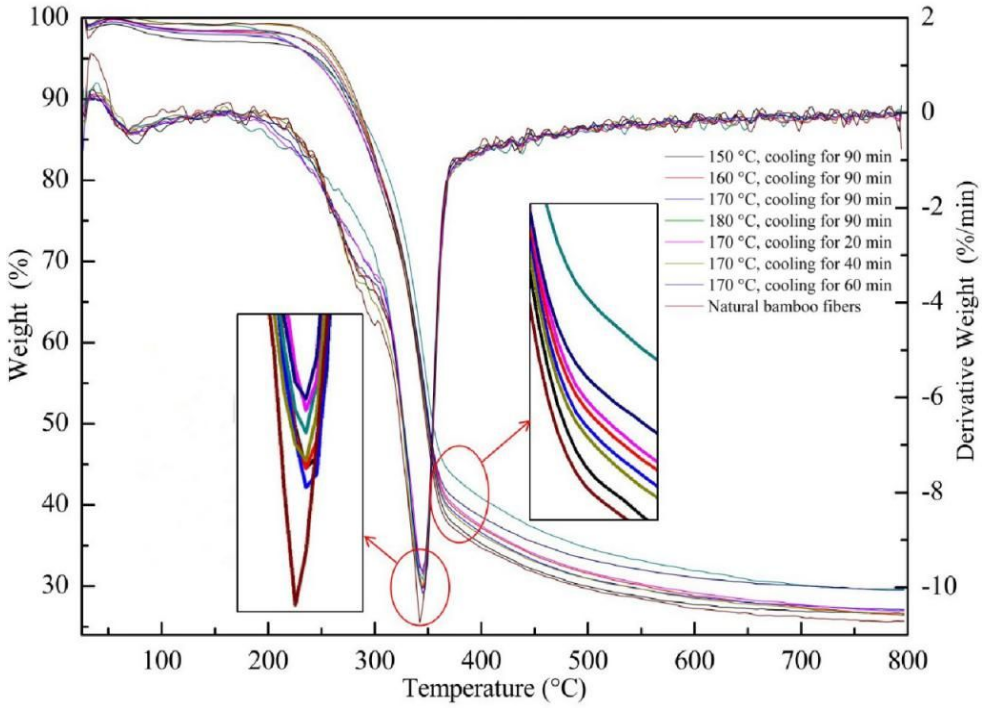

Figure S1. TGA/DTG curves of natural bamboo fiber and bamboo bio-composite.

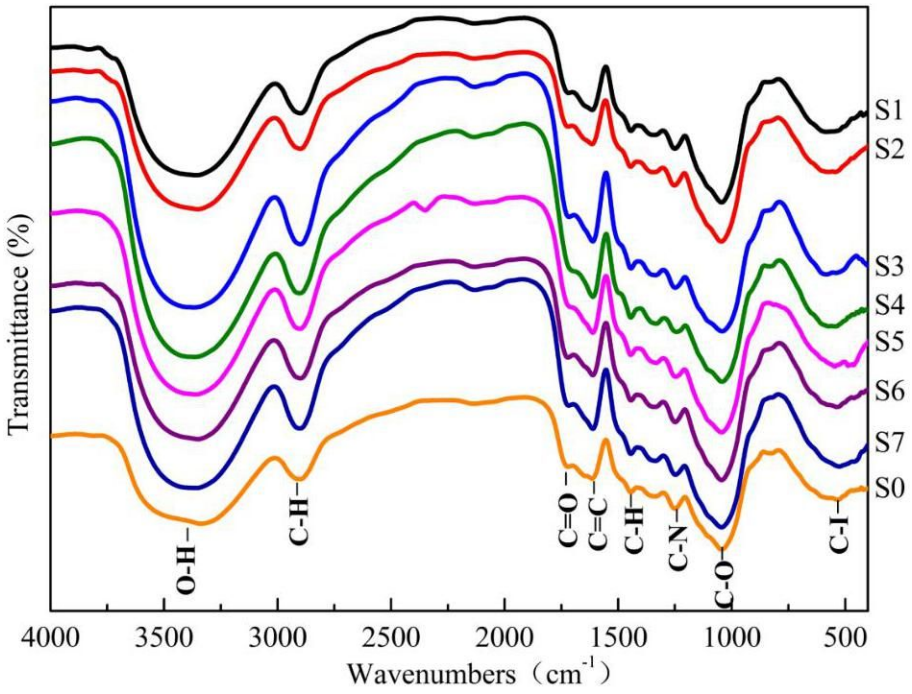

Figure S2. Infrared spectrum of natural bamboo fiber and bamboo bio-composite.

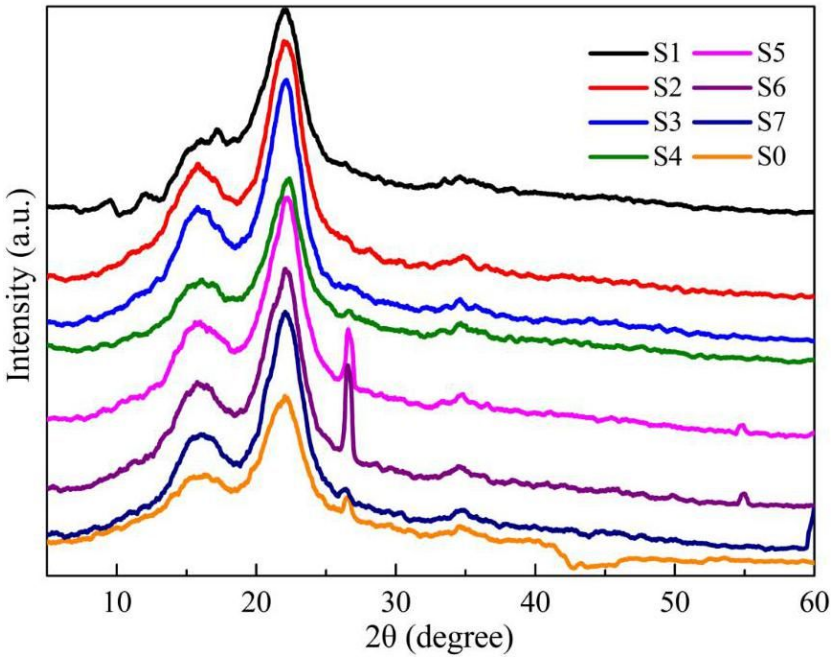

104

105 **Figure S3.** XRD curve of natural bamboo fiber and bamboo bio-composite.

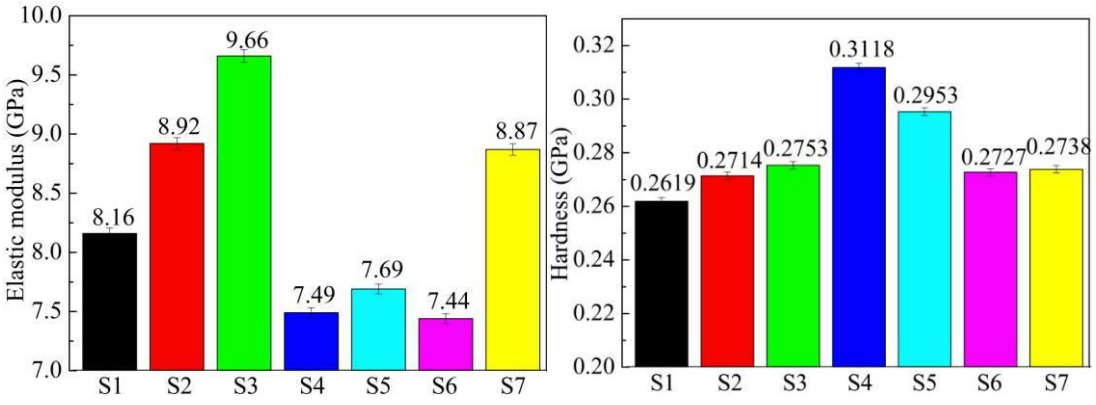

106

107 **Figure S4.** The elastic modulus and hardness of bamboo bio-composite.

s1

s2

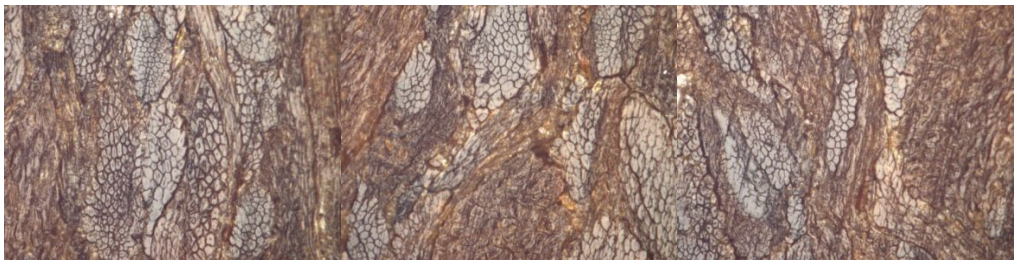

s3

s4

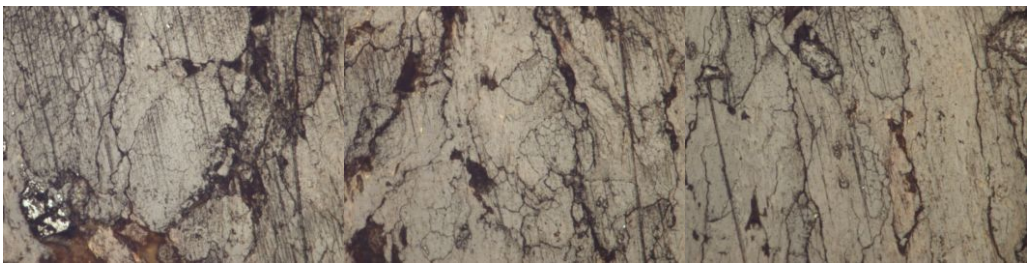

s5

s6

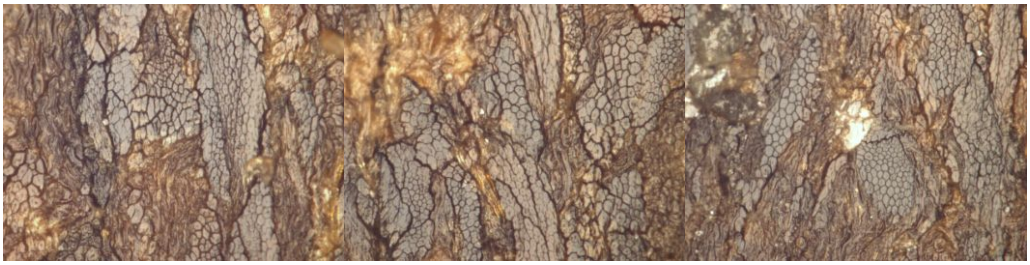

s7

Figure S5. Light microscopic photograph of bamboo bio-composite (S1-S7) by nanoindentation.

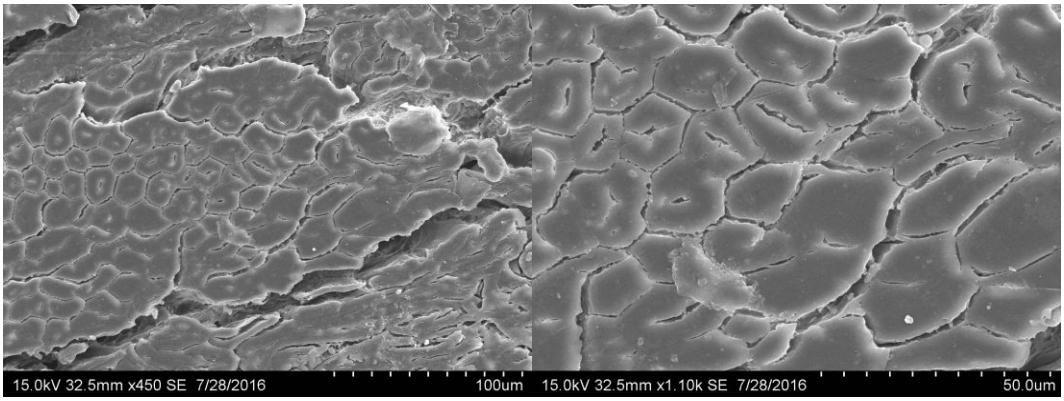
15.0kV 32.5mm x450 SE 7/28/2016
100um
15.0kV 32.5mm x1.10k SE 7/28/2016
50.0um

s1

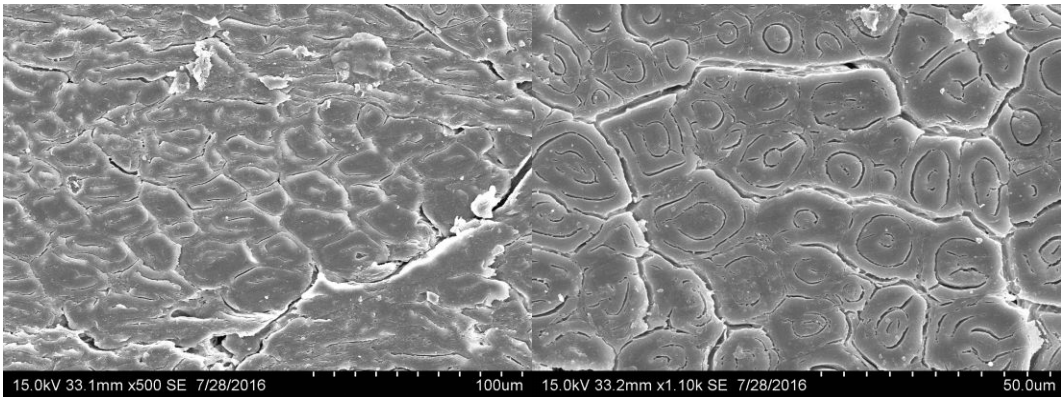
15.0kV 33.1mm x500 SE 7/28/2016
100um
15.0kV 33.2mm x1.10k SE 7/28/2016
50.0um

s2

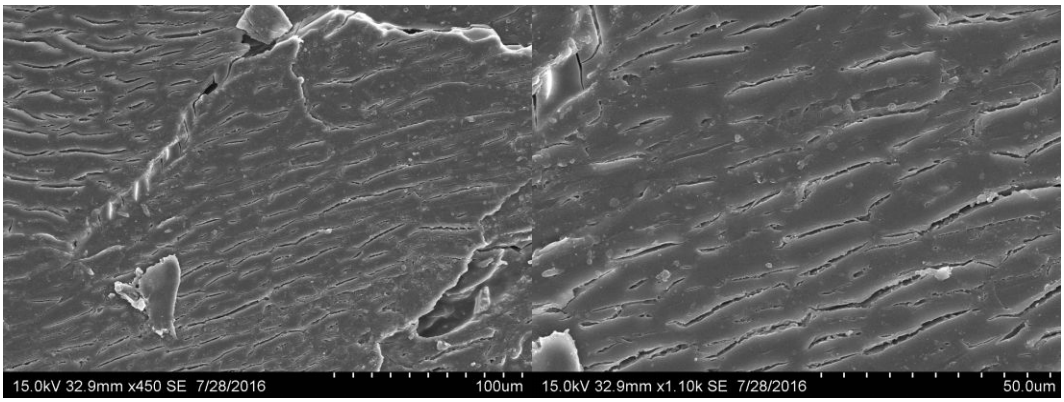
15.0kV 32.9mm x450 SE 7/28/2016
100um
15.0kV 32.9mm x1.10k SE 7/28/2016
50.0um

s3

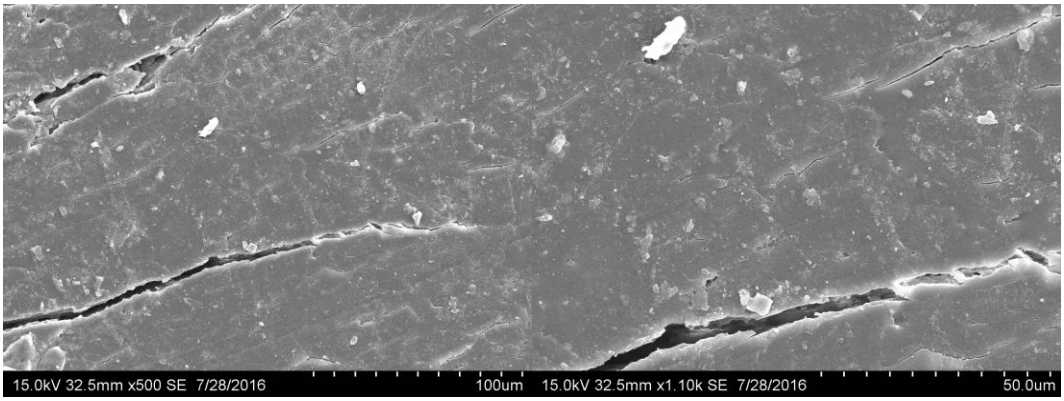
15.0kV 32.5mm x500 SE 7/28/2016
100um
15.0kV 32.5mm x1.10k SE 7/28/2016
50.0um

s4

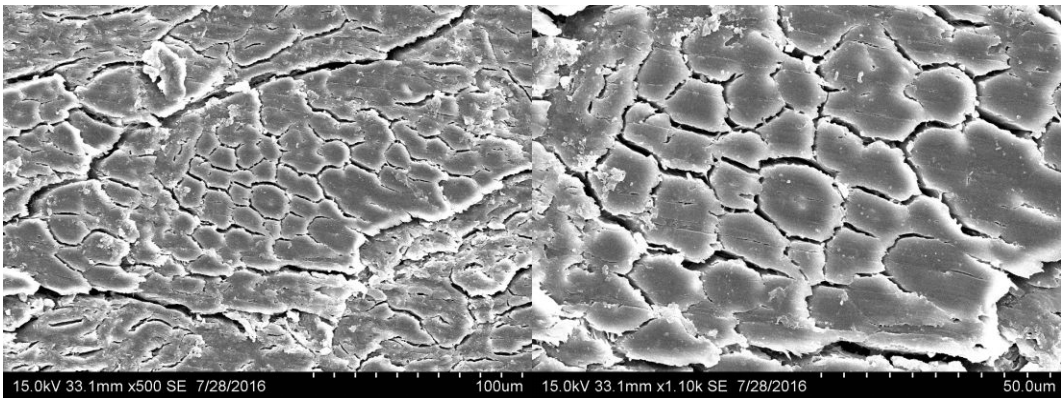
15.0kV 33.1mm x500 SE 7/28/2016
100um
15.0kV 33.1mm x1.10k SE 7/28/2016
50.0um

s5

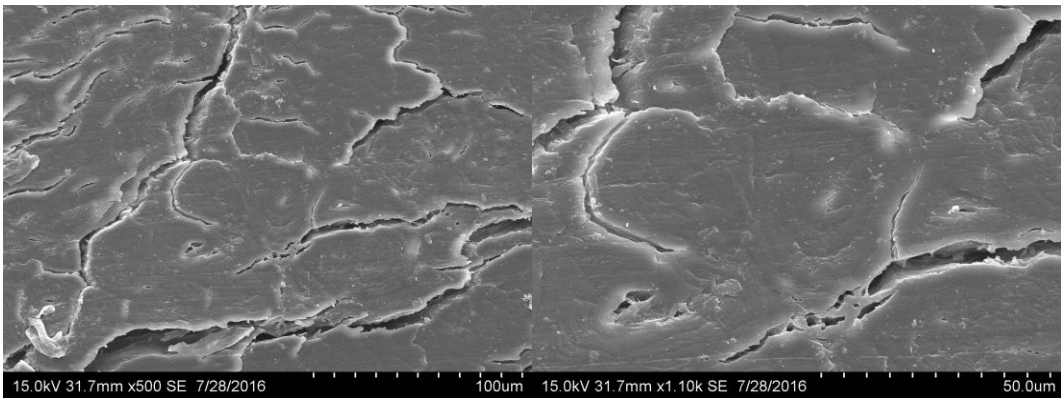
15.0kV 31.7mm x500 SE 7/28/2016
100um
15.0kV 31.7mm x1.10k SE 7/28/2016
50.0um

s6

141 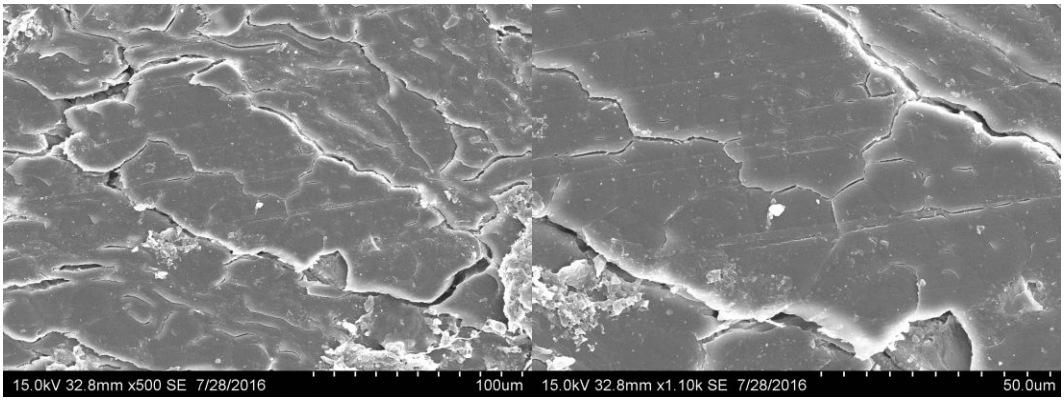

142 s7

143 **Figure S6.** Photograph of bamboo bio-composite surface (S1-S7) by SEM.

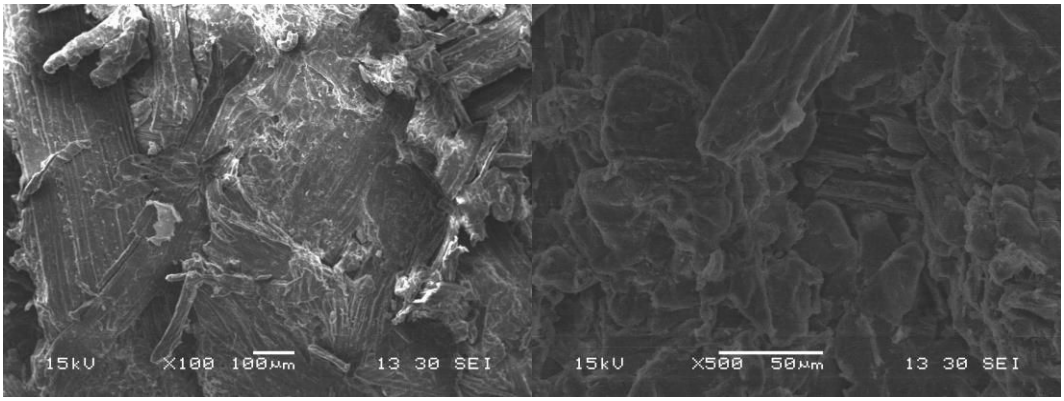
15kV X100 100µm 13 30 SEI
15kV X500 50µm 13 30 SEI

s1

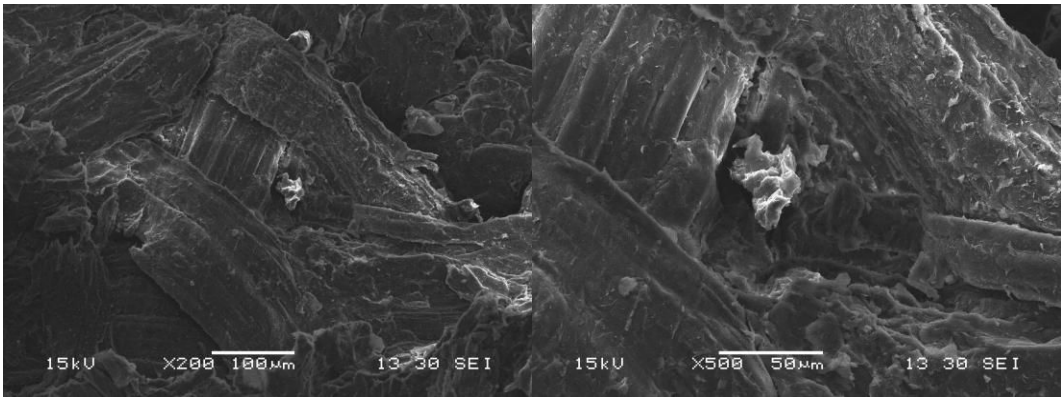
15kV X200 100µm 13 30 SEI
15kV X500 50µm 13 30 SEI

s2

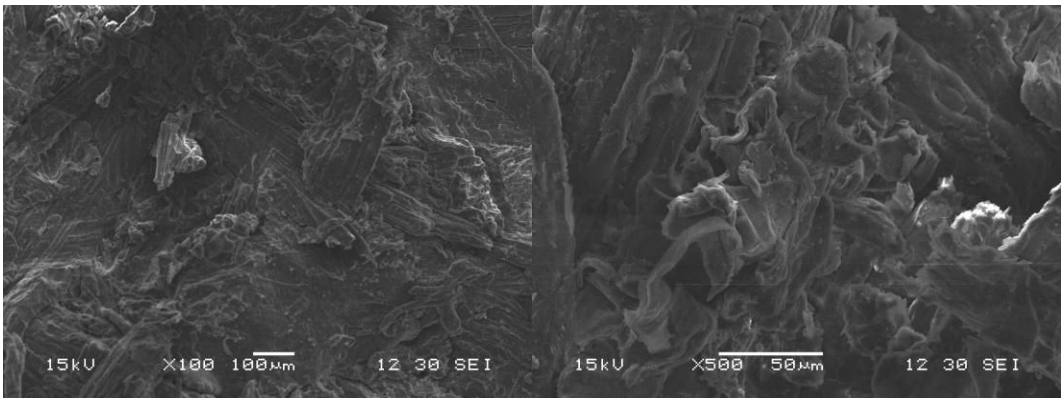
15kV X100 100µm 12 30 SEI
15kV X500 50µm 12 30 SEI

s3

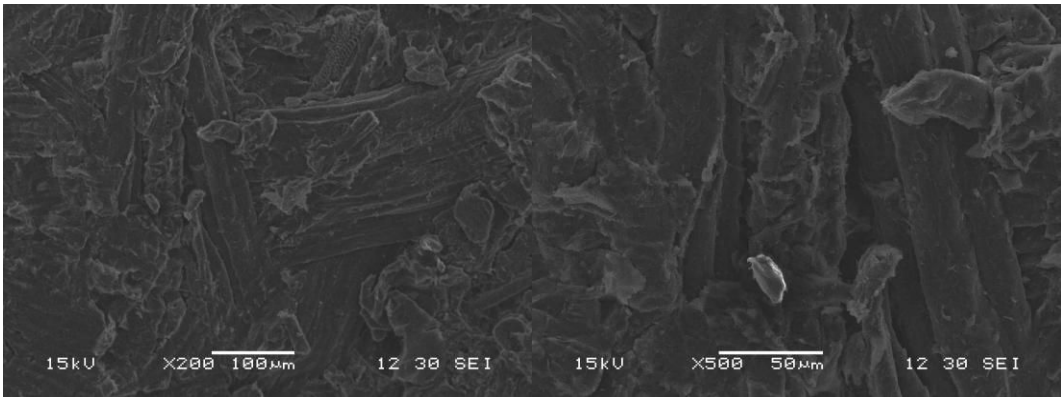
15kV X200 100µm 12 30 SEI
15kV X500 50µm 12 30 SEI

s4

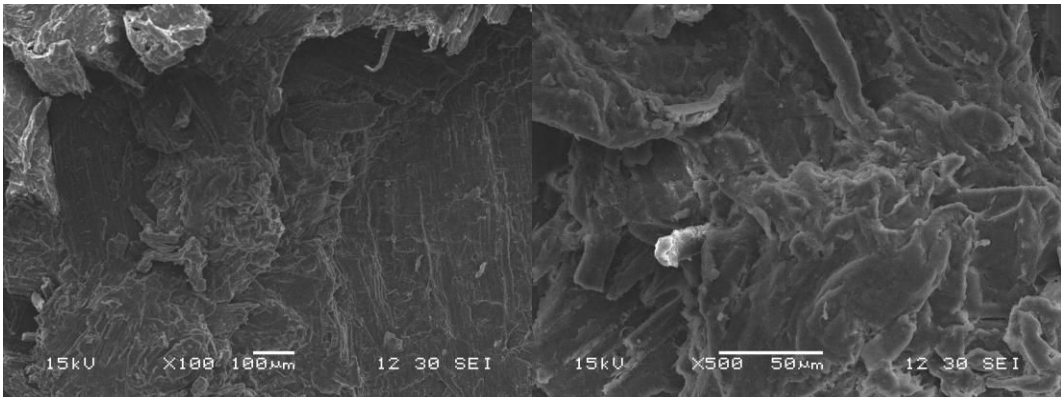
15kV X100 100µm 12 30 SEI
15kV X500 50µm 12 30 SEI

s5

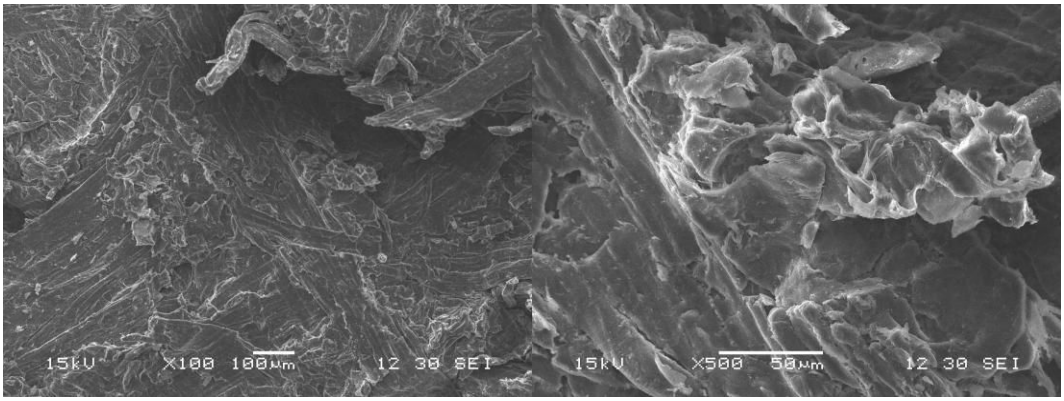
15kV X100 100µm 12 30 SEI
15kV X500 50µm 12 30 SEI

s6

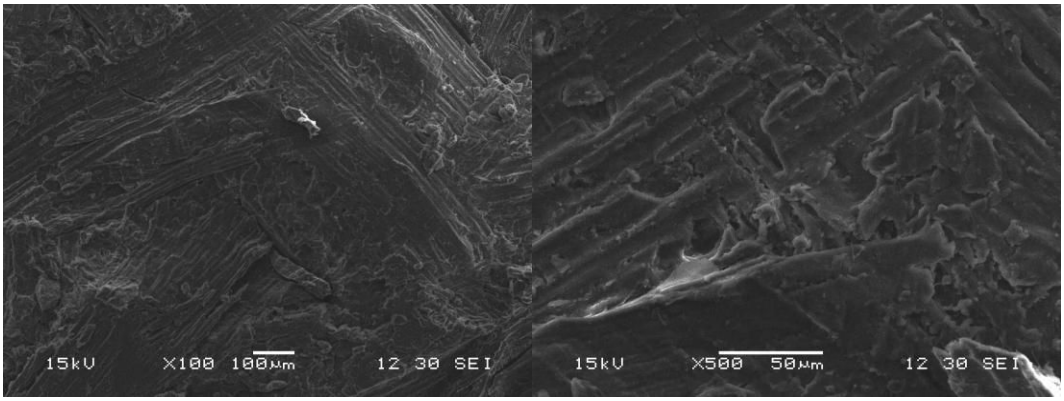

s7

Figure S7. Photograph of bamboo bio-composite (S1-S7) section by SEM.

159 **Table S1.** High thermal stability data of natural bamboo fiber and bamboo bio-composite.

No.	PHRR ($kW \cdot m^{-2}$)	THR ($MJ \cdot m^{-2}$)	PSPR ($m^2 \cdot s^{-1}$)	TSP (m^2)	CO ($g \cdot s^{-1}$)	CO_2 ($g \cdot s^{-1}$)
S1	117.92	29.31	0.023	0.836	0.0020	0.074
S2	133.22	27.03	0.035	1.824	0.0038	0.084
S3	167.25	35.24	0.015	2.250	0.0028	0.108
S4	156.49	35.80	0.013	1.302	0.0026	0.103
S5	164.37	32.47	0.023	1.043	0.0037	0.099
S6	136.43	25.50	0.023	0.998	0.0036	0.090
S7	139.23	27.53	0.027	1.746	0.0039	0.092
S0	128.84	26.29	0.025	0.755	0.0030	0.083

Table S2. Assignment of bands in FTIR spectrum of the bamboo fiber and bamboo bio-composite [39].

Compounds detected	Wavenumbers (cm^{-1})
O−H stretching vibration of aromatic and aliphatic groups	3389
C−H stretching vibration of CH_3, $-CH_2-$ and −CH− groups	2902
C=O stretching vibration of aldehydes, ketones, carboxylic acids, esters	1730
C=C stretching vibration of alkanes	1612
C−H stretching vibration of alkanes	1444
C−N stretching vibration of amines and amides	1242
C−O stretching vibration of aldehydes, ketones, carboxylic acids and esters	1034
C−I stretching vibration of aliphatic iodo compounds	553

Table S3. Distribution of bamboo resources in the world.

(Bamboo industry)	(Area) Khm^2	Eco-economic benefits （million USD）	Wood-Based Panels (million m^3)
Asia Pacific Region	11000 [40,41]	37378.15	320
American region	10200 [40,41]	34659.74	47.715
African region	1500 [40,41]	5097.02	3.469
European region	No or little natural bamboo	N/A	85.822

Note: Calculation basis of ecological and economic benefits [5-9]: CO_2 absorption about 170.91 T/ hm^2, 12.36 USD/ T; O_2 release: about 12 T/ hm^2, 57.14 USD/ T; reduce soil erosion: 30 t/ hm^2, 1.14 USD/ T; SO_2 absorption: About 9.9 T/ hm^2, 57.14 USD/ T. Ecological and economic benefits of 1 hm^2 bamboo = 3398.014 USD. Wood-Based Panels such as plywood, medium density fiberboard (MDF) and particleboard and the resins used like urea-formaldehyde (UF), melamine-modified urea formaldehyde (MUF), and phenol-formaldehyde(PF) are the main sources for FE. The present importance of such problematic results arises from the fact that formaldehyde was the first among the six chemical substances considered as industrial hazards (Tanabe,2008). In 2001, the CARB initiated the development of a regulation to reduce public exposure to formaldehyde. The CARB regulation, effective January 1, 2009, placed limits on formaldehyde emission (FE) from wood-based panels.

175 **Table S4.** Wood-Based Panels made by wood, bamboo, straw, branch and other wooden materials.

	Bonding strength (MPa)	**Water resistance (%)**	**Formaldehyde Emission** [47-53]
bamboo bio-composite	4.1	2	Near zero
fast-growing grass bio-composite	1.6	6	Near zero
poplar bio-composite	2	5	Near zero
American National Standards Institute (ANSI) A208.1-1999 Particleboard [17]	0.6	8	17.0mg/ 100g (0.6 mg/L)
American National Standards Institute (ANSI) A208.2-2002 Medium Density Fiberboard [18]	0.8	10	
China National Standard (CNS) GB/T 4897-2015 Particleboard [19]	0.4	8	15.0mg/ 100g (1.5 mg/L)
China National Standard (CNS) GB/T 11718-2009 Medium Density Fiberboard [20]	0.6	20	

176